Available online at www.sciencedirect.com
SCIENCE DIRECT®
ELSEVIER
Ocean Engineering 32 (2005) 685–700
OCEAN ENGINEERING
www.elsevier.com/locate/oceaneng

Technical note

Maximum output of an OTEC power plant

Rong-Hua Yeh*, Tar-Zen Su, Min-Shong Yang

Department of Marine Engineering, National Taiwan Ocean University, 2, Pei Ning Road, Keelung 202, Taiwan, ROC

Received 2 April 2004; accepted 11 August 2004
Available online 2 December 2004

Abstract

This paper theoretically investigates the effects of the temperature and flowrate of cold seawater on the net output of an OTEC plant. Parameters of pipe length, pipe diameter, seawater depth, and the flowrate of seawater are considered. It shows that a maximum output of the net work exists at a certain flowrate of cooling seawater. The output work is higher for a larger ratio of warm to cold seawater flow rate. For a lower cold seawater temperature, the maximum net output and the corresponding required flow rate of cold seawater becomes larger. The pipe diameters corresponding to maximum net output increase with decreasing cold seawater temperature for fixed flow velocity in pipes. In addition, a larger maximum net output can be obtained by employing a higher temperature of the surface warm seawater.

Keywords: OTEC; Maximum output; Network

1. Introduction

Due to the remarkable economic growth in Taiwan, the demand for electric power increases and the quality of life and health for the people deteriorates. For this reason, more and more researches are devoted to investigating the inexhaustible source of non-pollution energy. The water along the east coast of Taiwan is in the route of Kuroshio's major flow. The temperature difference between the surface water and that at 800 m deep is greater than

* Corresponding author.
E-mail address: rhyeh@mail.ntou.edu.tw (R.-H. Yeh).

0029-8018/$ - see front matter © 2005 Elsevier Ltd. All rights reserved.
doi:10.1016/j.oceaneng.2004.08.011

Nomenclature

A	heat transfer area
c_p	specific heat
D	pipe diameter
F	correction factor, Eq. (1)
f	friction factor or fouling factor
h	heat transfer coefficient or enthalpy
g	acceleration of gravity
k	thermal conductivity
L	pipe length
m	mass flow rate
P	pressure
Pr	Prandtl number
Q	heat transfer rate
Re	Reynolds number
r	radius
s	entropy
T	temperature
U	overall heat transfer coefficient
V	velocity
v	specific volume
W	work
x	quality

Greek letters

α	ratio of liquid ammonia to mixture in the evaporator
β	ratio of liquid ammonia to the whole mixture of the working fluid
η	efficiency
ν	kinematic viscosity of working fluid
ρ	density

Subscripts

a	ammonia
c	condenser or condensing
ci	inlet of the condenser
co	outlet of the condenser
cs	deep cold seawater
e	evaporator or evaporating
ei	inlet of the evaporator
eo	outlet of the evaporator
fg	difference between saturated vapor and saturated liquid
g	generator
h	hydraulic diameter of heat exchanger (condenser and evaporator)

i	inner
l	liquid
lm	log mean
m	mean or average
n	generated net power
o	outer
p	pumping
t	tube or turbine
to	exit of the turbine
v	vapor
w	seawater
ws	warm seawater
s	solid wall or storage tank

20 °C most of the time through a year in this area. It makes this area possessing superior potential to develop OTEC (Ocean Thermal Energy Conversion) energy resources.

It is known that the deeper the cooling water is pumped from the sea, the more efficient will the OTEC plant work. Besides, an additional benefit of this system will be an enormous amount of pathogen-free and nutrient-rich cold seawater pumped up from the deep sea. This water can be used for the culture of high value marine-cultural cops, refrigeration, air-conditioning, and production of potable water (Dylan, 1995). However, the riskiest part of construction for the seawater system will be the cold water pipe. Laying pipes to greater depth may lead to higher pumping head requirements and needs higher costs (Avery and Wu, 1994).

The OTEC power plant uses the heat in the surface water of the tropical oceans to generate electricity and uses cold water drawn from deep sea to cool and liquefy the vapor emerging from the turbine. Since D'Arsenoval conceived the OTEC concept in 1881, and Laude first implemented the data and idea in 1930, there has been a wide range of interest in OTEC technology.

A lot of research efforts were engrossed in the performance improvement of an OTEC plant due to its low efficiency. Using freon 22 as a working fluid, Uehara et al. (1979) studied the performance of an OTEC plant. Later, Nakaoka and Uehara (1988a,b) conducted experiments to test the performance of an OTEC system with shell-and-plate-type evaporator and condenser. In addition, Ganic and Moeller (1980) carried out the performance study of an OTEC plant. Owens (1980) investigated the optimization of closed-cycle OTEC plants. Using ammonia as the working fluid, an optimization study by Power method was presented by Uehara and Ikegamia (1990) for a closed-cycle OTEC plant. Both constant and variable turbine efficiencies were considered in their study. Later, Rabas et al. (1990) proposed a comprehensive study of the non-condensible gas removal system for a particular 10 MW hybrid power plant. Dividing the power plant into three major subsystems, Tseng et al. (1991) utilized an optimal design concept to find the best design for a complex and large-scale OTEC plant. Using the total heat transfer area of heat exchangers per net power as an objective function, an OTEC cycle with plate-type heat

exchangers and ammonia as working fluid was investigated numerically (Uehara et al., 1996). Recently, based on plate exchangers with surface coating on the ammonia side, Abraham et al. (1999) have proposed the design of 1 MW closed-cycle floating OTEC plant.

The difference in seawater temperature between the surface and deep ocean off eastern Taiwan is around 20 °C for the entire year. In addition, the east coast of Taiwan drops off rapidly so that the OTEC plant can be constructed on shore and still have a cold seawater pipe of reasonable length. The purpose of this study is to develop a computerized calculation method for the performance analysis of an OTEC plant. Parameters of pipe length, pipe diameter, warm and cold seawater temperature, mass flow rate of seawater are considered to obtain the generated net power. For practical applications, the seawater temperature–pipe length relationship (Yeh et al., 1999) of Taitung county, located in eastern Taiwan, is employed in the analysis.

2. Mathematical analysis

For a given evaporator or condenser, a shell-and-tube heat exchanger, the heat transfer rate between the working fluid and seawater can be expressed as

$$Q = UAF\Delta T_{\mathrm{lm}} \tag{1}$$

where Q is the total heat transfer, U stands for overall heat transfer coefficient, A is entire surface area, F is a correction factor, and ΔT_{lm} represents a log mean temperature difference of the evaporator or condenser. The overall heat transfer coefficient may be determined from knowledge of the hot and cold fluid convection coefficients, fouling factors, and appropriate geometric parameters. For a U based on the outside surface area of the heat exchanger, it may be written as

$$U = 1/[(A_{\mathrm{o}}/A_{\mathrm{i}})(1/h_{\mathrm{w}}) + (A_{\mathrm{o}}/h_{\mathrm{s}}) + (1/h_{\mathrm{m}}) + f_{\mathrm{o}}] \tag{2}$$

Note that subscripts i and o refer to inner and outer tube surfaces, which may be exposed to either the working fluid or the seawater, and f_{o} is the fouling factor of heat transfer surface. In Eq. (2), the heat transfer coefficient in the seawater side, h_{w}, for the transition case, $2300 < Re_{\mathrm{w}} < 10{,}000$, can be calculated from the empirical expression (Gnielinski, 1976)

$$h_{\mathrm{w}} = \left(\frac{k_{\mathrm{w}}}{D_{\mathrm{h}}}\right) \frac{(Re_{\mathrm{w}} - 1000)Pr_{\mathrm{w}}(f_{\mathrm{w}}/2)}{1 + 12.7(f_{\mathrm{w}}/2)^{0.5}(Pr_{\mathrm{w}}^{2/3} - 1)} \tag{3}$$

where

$$f_{\mathrm{w}} = [1.58\ln(Re_{\mathrm{w}}) - 3.28]^{-2} \tag{4}$$

and for the fully developed turbulent flow, i.e. $Re_{\mathrm{w}} > 10{,}000$, the Petukhov correlation (Petukhov et al., 1973) is used

$$h_{\mathrm{w}} = \left(\frac{k_{\mathrm{w}}}{D_{\mathrm{h}}}\right) \frac{Re_{\mathrm{w}}Pr_{\mathrm{w}}(f_{\mathrm{w}}/2)}{1.07 + 12.7(f_{\mathrm{w}}/2)^{0.5}(Pr_{\mathrm{w}}^{2/3} - 1)} \tag{5}$$

where k_w, f_w, Re_w, and Pr_w are the thermal conductivity, fanning friction factor, Reynolds number and Prandtl number of the seawater. In addition, D_h denotes the hydraulic diameter of the heat exchanger.

The conductance, h_s, of the tube wall may be written in the form

$$h_s = \frac{2\pi k_t L}{\ln\left(\frac{r_o}{r_i}\right)} \tag{6}$$

where k_t is the thermal conductivity, L is the length, r_o and r_i are the outer and inner radii of the tubes in the heat exchangers.

The heat transfer coefficient, h_m, in the side of working fluid has two different values depending on condensation or evaporation. In condenser, it is calculated as

$$h_m = 0.725\left[\frac{(\rho_l - \rho_v)g h_{fg} k_v}{D_h v (T_m - T_c)}\right]^{0.25} \tag{7}$$

where ρ, k and v are density, thermal conductivity and kinematic viscosity of working fluid at condensing temperature. Also, the average temperature outside the tubes is denoted as T_m, the condensing temperature is abbreviated as T_c, and h_{fg} is the enthalpy difference between saturated vapor and saturated liquid of the working fluid. As for an evaporator, it is given as

$$h_m = 0.62\left\{\frac{(\rho_l - \rho_v)g[h_{fg} + 0.4c_{pv}(T_m - T_c)]k_v}{D_h v (T_m - T_c)}\right\}^{0.25} \tag{8}$$

Note that the above thermal properties are obtained at evaporating temperature, and T_e is the evaporating temperature of the working fluid.

The total heat flow of the evaporator can be evaluated as

$$Q_e = m_{ws} c_{pw} (T_{ei} - T_{eo}) \tag{9}$$

In Eq. (9), m_{ws} and $\boldsymbol{c}_{pw}$ are mass flow rate and specific heat of the warm (surface) seawater temperatures, and T_{ei} and T_{eo} are the inlet and outlet seawater temperatures of the evaporator, respectively. From energy balance, the quantity of circulating working fluid can be obtained as

$$m_a = Q_e/(h_{eo} - h_{ei}) \tag{10}$$

where h_{eo} and h_{ei} are the enthalpies of working fluid at the outlet and inlet temperatures of the evaporator.

To simulate the real cases, it is assumed that a certain portion of the working fluid returns to the storage tank and the rest goes to the generator and enters the condenser. Suppose that the working fluid changes from saturated vapor into saturated liquid isothermally. The heat transfer rate of the condenser can then be calculated as

$$Q_c = m_a(h_{ci} - h_{co}) \tag{11}$$

or alternatively

$$Q_c = m_{cs} c_{pw} (T_{co} - T_{ci}) \tag{12}$$

The output of the turbine work can be evaluated by assuming that the saturated vapor of the working fluid expands isentropically into low pressure's mixture of saturated vapor and liquid. In this case, the quality of ammonia vapor leaving the turbine can be obtained as

$$x = (s_{to} - s_{co})/(s_{ci} - s_{co}) \tag{13}$$

where s_{to} is the entropy of the working fluid at the exit of the turbine, and s_{co} and s_{ci} are the entropies of saturated liquid and saturated vapor at condensing temperature. The enthalpy of the working fluid vapor at the outlet of the turbine therefore becomes

$$h_{to} = (1 - x)h_{ci} + xh_{co} \tag{14}$$

In the above equation, h_{ci} and h_{co} are the enthalpies of saturated liquid and saturated vapor at the temperature of condensation. Since the enthalpies at the entrance and exit of the turbine are known, the total electric work resulting from turbine can be calculated as

$$W_t = m_a (h_{eo} - h_{to}) \eta_t \eta_g \tag{15}$$

where h_{eo} is the enthalpy of saturated vapor at evaporating temperature, and η_t and η_g are efficiencies of turbine and generator, respectively.

For an isentropic process, the power consumption of the working fluid circulating pump can be expressed as

$$W_a = m_a v_a [(P_{ei} - P_{eo}) + (\alpha + \beta)(P_{ei} - P_s)]/\eta_p \tag{16}$$

In Eq. (16), v_a is the specific volume of saturated liquid working fluid at condensing temperature, P_{ei} and P_{eo} are the pressure of working fluid at evaporating and condensing sides, respectively, P_s is the pressure of storage tank of working fluid and η_p is the efficiency of circulating pump. In addition, α is the ratio of liquid ammonia to mixture as the working fluid flow through the evaporator whereas β is ratio of liquid ammonia, which did not evaporate in the evaporator, to the whole mixture of the working fluid. In this study, both α and β are assumed to be 0.125.

The OTEC system utilizes cold seawater in the deep sea for cooling and warm seawater from the sea surface as a heating source. Therefore, some of the generating electric works are required for pumping water from sea to the plant. The power consumption of the pump is mainly to overcome the friction loss as seawater goes through the pipes, fittings, and heat exchangers. The summation of all the pressure losses caused by the friction between seawater and pipe wall or fitting can be given as

$$\Delta P_s = \sum_{i=1}^{n} f_i V^2 L_i/(2gD_i), \quad i = 1, 2, 3, \ldots, n \tag{17}$$

where f_i is the friction factor of pipe or fitting, V is the velocity of seawater, L_i is the pipe length, and D_i is the diameter of pipe. Considering the core friction, the pressure drop

associated with seawater flow through an evaporator or a condenser is given by

$$\Delta P_h = \rho V^2 \left(\frac{f_h}{2}\right)\left(\frac{D_h}{A_h}\right)\left(\frac{L_h}{g}\right) \tag{18}$$

In Eq. (18), ρ and V are the density and velocity of seawater, f_h, D_h, A_h, and L_h are the friction factor, diameter, cross-sectional area and length of the tubes used in evaporators or condensers.

The total power required for the surface warm as well as the deep cold seawater pump then becomes

$$W_s = (\Delta P_s + \Delta P_h) m_s g/\eta_s \tag{19}$$

where m_s is the flow rate of the seawater and η_s signifies the efficiency of seawater pump. The net power W_n is calculated from

$$W_n = W_t - W_{ws} - W_{cs} - W_p \tag{20}$$

In the above equation, W_t is the generated turbine power, W_{ws} is the warm seawater pumping power, W_{cs} is the cold seawater pumping power, and W_p is the pumping power of the working fluid.

3. Solution procedures

In this study, several parameters are known and are listed as follows:

1. the temperature of the surface warm seawater T_{ei} and deep cold seawater T_{ci}.
2. the diameter D, length L, wall thickness t and number of tubes N used in evaporators or condensers.
3. the efficiencies of working fluid circulating pump, seawater pumps, and turbine generator.
4. friction factor, fouling factor, and liquid ratios of the working fluid.

With the above given values, the total surface area of heat exchangers and some dimensionless parameters can be calculated. Subsequently, the heat transfer coefficients inside and outside the tubes in evaporator are obtained. The overall heat transfer coefficient is then determined from Eq. (2). This analysis initiates with the assumption of the outlet temperature of warm seawater in evaporator. With the aid of Eq. (1), the heat transfer rate of the evaporator can be computed. Also, from Eq. (9), the heat dissipated by warm seawater can be evaluated. An iteration method with updating T_{eo} continues until a specified tolerance of 0.001 (relative error) is met. As the heat duty of evaporator is calculated, the quantity of working fluid can be obtained from Eq. (10). In a similar manner, the heat flow of the condenser and the outlet of cold seawater are found from Eqs. (1) and (12). In addition, the pressure drops of pipes, fitting, and heat exchanger can be determined from Eqs. (17) and (18). The power consumed by the seawater pumps and working fluid pump can then be calculated. The net output of the turbine work is finally found from Eq. (20). Detailed flow chart of the calculation is given in Fig. 1.

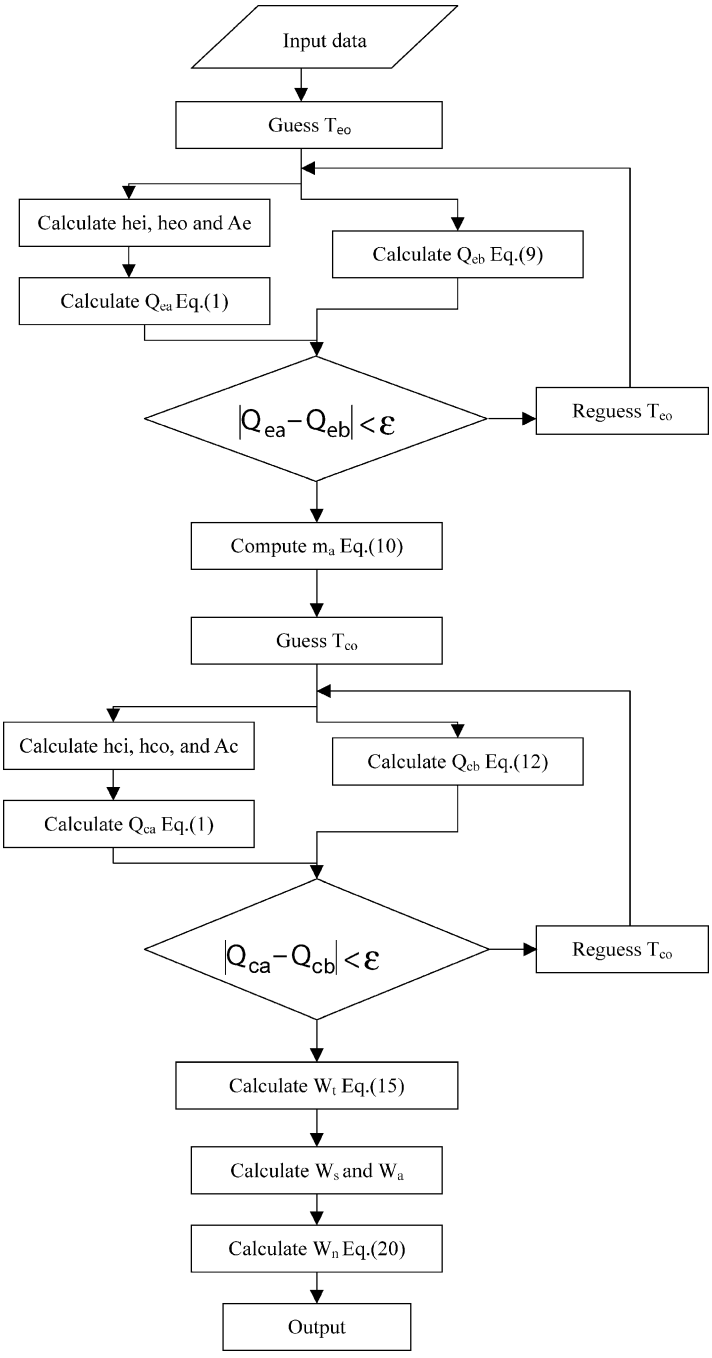

Fig. 1. Flow chart of calculation.

Table 1
Depth–temperature relationship and actual pipe length used in this study

Depth of sea (m)	Temperature (°C)	Horizontal distance (m)	Actual pipe length (m)
500	8	2900	3200
600	7	3100	3400
700	6	3600	4000
800	5	4100	4500

4. Results and discussion

In this study, it is assumed that the OTEC plant is situated in Taitung county, east cost of Taiwan. For the first part, the surface warm water temperature is 25 °C and the cold seawater temperatures are specified as 5–8 °C. In the latter part, the cold seawater temperature is assumed 5 °C whereas the warm seawater temperatures are 20, 25, 30, and 35 °C, respectively. The relationship between deep cold water temperatures and actual pipe lengths are shown in Table 1. The OTEC system converts heat energy into electricity by using the temperature difference between water at the surface of the ocean and cold water of the depths. The larger the temperature difference is, the higher the plant efficiency will be. However, in practical applications, it is observed that the lower the seawater temperature is, the longer the piping is needed in Table 1. The increase in the turbine work is offset by the pumping power of cold seawater. Thus, a computerized calculation method is developed to find the appropriate design conditions with which maximum net output power is produced. Table 2 lists the design parameters used in computation. Ammonia is selected as the working fluid. Both evaporator and condenser of this plant are shell-and-tube exchangers, in which the tubes are made of stainless steel. The heat transfer area of the condenser is the same as that of the evaporator. Although various seawater pipe diameters are given for calculation, identical pipe diameters for evaporators and condensers are used in each run. For practical applications, the surface warm seawater pipe is much shorter than the deep cold seawater pipe.

Table 2
Parameters of the proposed OTEC plant

Parameters	Values
Warm seawater pipe length (m)	250
Thermal conductivity of heat exchangers (W/m K)	14
Turbine efficiency (%)	89
Seawater pump efficiency (%)	85
Working fluid pump efficiency (%)	85
Generator efficiency (%)	96
Warm seawater inlet temperature (°C)	20, 25, 30 and 35
Cold seawater inlet temperature (°C)	5, 6, 7 and 8
Seawater pipe diameter (Cold and warm) (m)	0.5, 1, 1.5 and 2

4.1. Fixed pipe diameters

Fig. 2 depicts the dependence of powers on the mass flow rate of cold seawater for $T_{ci}=8$ °C and $D_{cs}=1$ m. On the whole, W_t, W_n, W_{cs}, W_{ws}, and W_p increase with m_{cs}. Note that the pumping power of the working fluid and the warm seawater pumping power in a OTEC plant system play an insignificant role in the determination of net power. This is because the required pipe lengths are smaller for warm seawater and working fluid in this system. The pressure loses caused by the friction between fluids and pipe walls or fittings are thus smaller. For a fixed pipe diameter, the mass flow rate of the cooling water increases with the flow velocity of cold seawater. Since the pumping power is proportional to the third power of V_{cs}, W_{cs} rises very quickly with m_{cs}. For this reason, a maximum net power can be obtained at an appropriate mass flow rate of seawater. A further increase in m_{cs}, the total sum of W_{cs}, W_{ws}, and W_p may be larger than W_t and W_n will even become negative. In this case, the generated turbine power is not enough to sustain the total pumping powers of the seawater and working fluid. The dependence of powers on the mass flow rate of cold seawater for $T_{ci}=5$ °C and $D_{cs}=1$ m is shown in Fig. 3. Viewing the two figures, similar phenomenon is observed. For the same system, as the cooling seawater temperature is changed from 8 to 5 °C, apparent increases in W_t, W_n, W_{cs}, W_{ws}, and W_p can be observed. Also, note that the increasing rate of the working fluid pumping power for $T_{ci}=5$ °C is larger than that for $T_{ci}=8$ °C. This is due to the fact that the evaporating and condensing temperatures of the working fluid are fixed, for energy balance a larger mass flow rate of the working fluid is needed for a lower temperature of seawater temperature. The working fluid thus has an obvious increase in pumping power especially at a larger m_{cs}. In addition, the maximum net power of the OTEC plant increases from 112 kW for $T_{ci}=8$ °C to 248 kW for $T_{ci}=5$ °C whereas the corresponding seawater flow rate merely

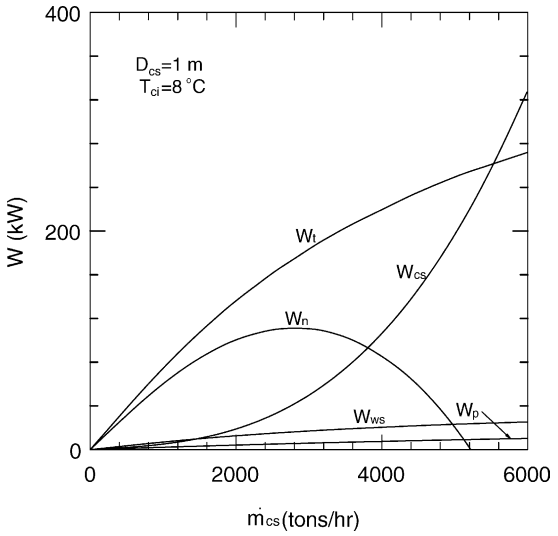

Fig. 2. Dependence of W_t, W_n, W_{cs}, W_{ws}, and W_p on m_{cs} for $T_{ci}=8$ °C.

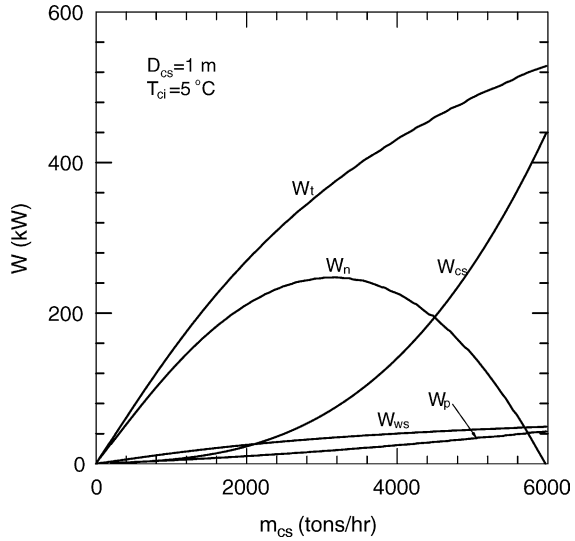

Fig. 3. Dependence of W_t, W_n, W_{cs}, W_{ws}, and W_p on m_{cs} for $T_{ci}=5$ °C.

increases from 2800 to 3200 tons/h. It is interesting to see the effects of T_{ci} on W_n for $D_{cs}=1$ m and $T_{ei}=25$ °C. Fig. 4 plots the dependence of W_n on m_{cs} for $T_{ci}=5$, 6, 7 and 8 °C and for $D_{cs}=1$ m and $T_{ei}=25$ °C. In this figure, $(W_n)_{max}=112$, 160, 204, and 248 kW for $T_{ci}=8$, 7, 6, and 5 °C, respectively. Although apparent increases in net powers are obtained, no pronounced increase in the corresponding m_{cs} is found. This can be explained

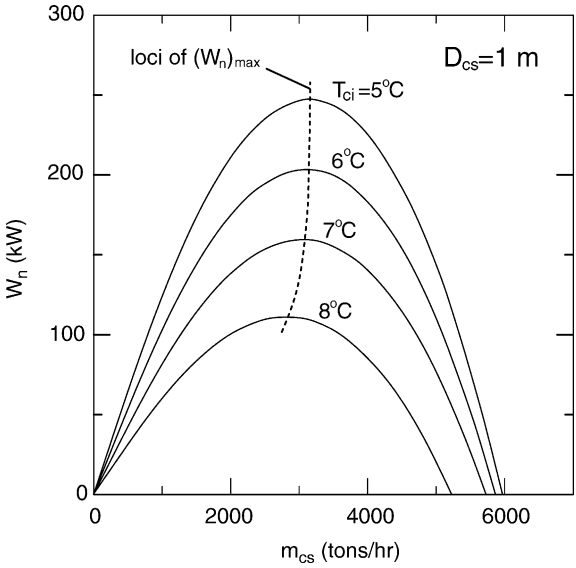

Fig. 4. Dependence of W_n on m_{cs} for $T_{ci}=5$, 6, 7, and 8 °C.

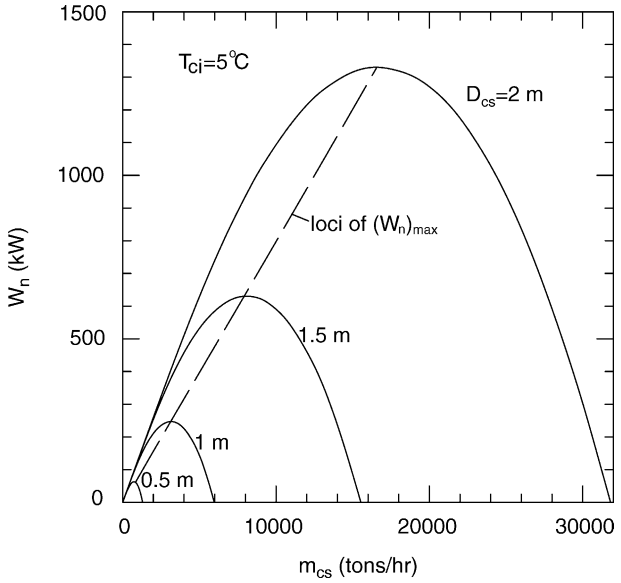

Fig. 5. The effects of seawater pipe diameters on W_n for $T_{ci}=5$ °C.

that a larger temperature difference between heat source and sink results in a high efficiency of OTEC plant. The loci of $(W_n)_{max}$ is also included in this figure. Fig. 5 displays the dependence of W_n on m_{cs} for $D_{cs}=0.5$, 1, 1.5, and 2 m and $T_{ci}=5$ °C. By increasing V_{cs} of cooling seawater, the mass flow rate can be increased for a fixed pipe diameter. It is shown that the maximum net power increases from 63 kW for $D_{cs}=0.5$ m to 1334 kW for $D_{cs}=2$ m. Thus, it is effective to increase $(W_n)_{max}$ by utilizing a larger pipe. However, the required corresponding m_{cs} to $(W_n)_{max}$ also increases enormously. The dependence of $(W_n)_{max}$ on T_{ci} for $D_{cs}=0.5$, 1, 1.5, and 2 m is given in the lower portion of Fig. 6. As a whole, $(W_n)_{max}$ decreases with T_{ci}. At a specified T_{ci}, the maximum net power is larger for a larger pipe of seawater. The required corresponding mass flow rate of cooling seawater to $(W_n)_{max}$ is shown in upper portion of Fig. 6. No pronounced variation of m_{cs} is observed for T_{ci} below 7 °C. The mass flow rate of seawater tends to decrease for T_{ci} greater than 7 °C. Nevertheless, the maximum net power becomes lower for a higher T_{ci}. This figure also sets up a guideline for piping design. It is suggested that the mass flow rate of cooling seawater should not exceed the proposed limit for a specified pipe diameter used otherwise W_n will decrease with increasing m_{cs}. This can be understood from the observation of Figs. 2–5. Fig. 7 describes the effects of m_{cs} on W_n for various $T_{ci.}$ when m_{cs} is lower than the design limit of m_{cs}, i.e. the mass flow rate of seawater corresponding to $(W_n)_{max}$. As expected, the net power decreases with increasing T_{ci}. In addition, W_n is larger for a larger m_{cs} at a given T_{ci}.

There is still an alternative way to increase net power if the mass flow rate of cold seawater is fixed. Fig. 8 shows the dependence of W_n on m_{ws}/m_{cs} for $T_{ci}=5$ °C and $D_{cs}=2$ m. It is apparent that W_n increases with m_{ws}/m_{cs}. From Figs. 7 and 8, W_n

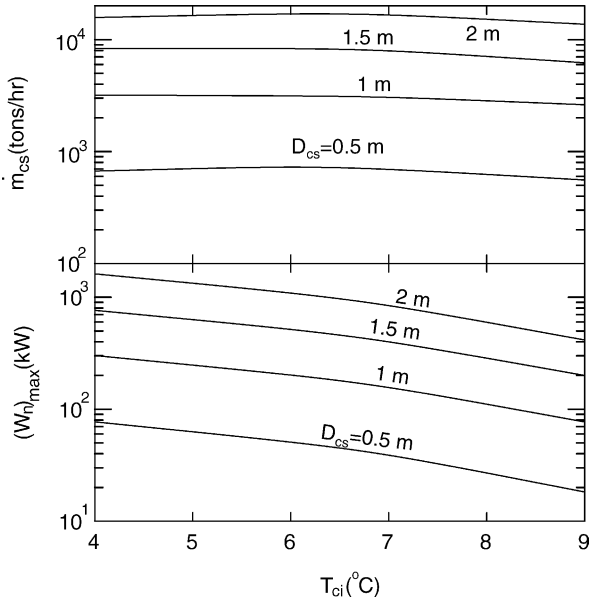

Fig. 6. The effects of seawater pipe diameter on $(W_n)_{max}$ and m_{cs}.

increases from 500 kW for $m_{ws}=4000$ tons/h to 540 kW for $m_{ws}=4400$ tons/h. This is because the evaporating temperature rises due to the increase in the mass flow rate of warm seawater. The performance of the OTEC plant is, therefore, improved.

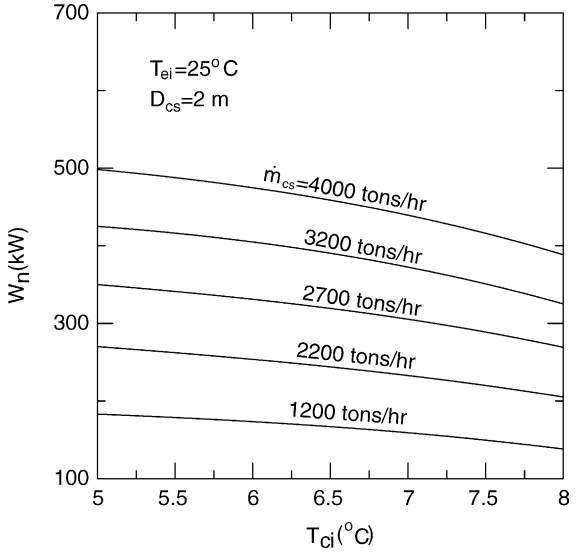

Fig. 7. Dependence of net power on the temperature of cold seawater.

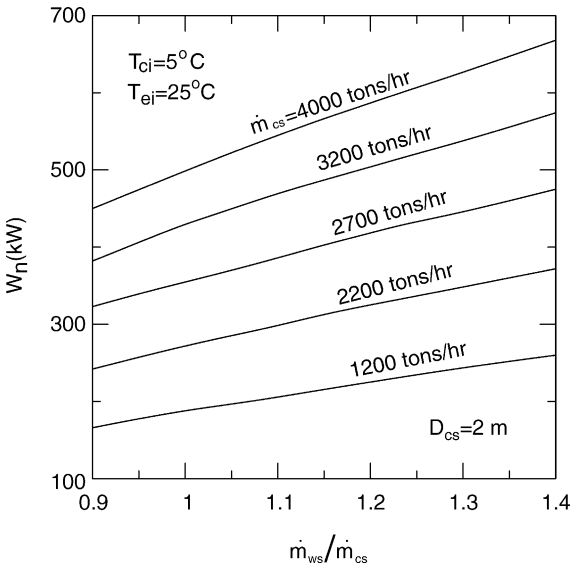

Fig. 8. Dependence of W_n on m_{ws}/m_{cs} for $T_{ci}=5$ °C, $T_{ei}=25$ °C, and $D_{cs}=2$ m.

In any case, the expense in increasing m_{ws} is lower than m_{cs} because the pipe for warm seawater is shorter than that of cold seawater. The pumping power, by all means, for the former is smaller due to lower friction loss.

4.2. Fixed flow velocities

To increase the mass flow rate, it can be achieved by accelerating the flow velocity for a fixed pipe diameter; or alternatively, by increasing the pipe diameter for a fixed flow velocity. For convenience, it is assumed that $V_{cs}=1$ m/s herein. Fig. 9(a) and (b) give the dependence of W_n on D_{cs} and m_{cs} for $T_{ei}=25$ °C and $V_{cs}=1$ m/s. Comparing Fig. 9(b) with Fig. 4, the maximum net power turns out to be a little lower for this case. It is clarified that the data in Fig. 4 is presented under the condition of $D_{cs}=1$ m and the flow velocities are all smaller than $V_{cs}=1$ m/s. Also, it should be emphasized that flow velocity plays a dominant role in pressure loss. The pumping power is thus higher for a larger V_{cs}. In Fig. 4, the seawater velocities corresponding to the maximum net powers are 0.38 m/s for $T_{ci}=8$ °C, 0.57 m/s for $T_{ei}=7$ °C, 0.77 m/s for $T_{ei}=6$ °C, and 0.97 m/s for $T_{ei}=5$ °C, respectively. From Fig. 9(a), it is shown that $(W_n)_{max}$ is obtained at a larger pipe diameter for a colder cooling seawater used for $V_{cs}=1$ m/s.

It is desirable to learn that the effect of T_{ei} on W_n for $V_{cs}=1$ m/s. Fig. 10(a) and (b) present the dependence of W_n on D_{cs} and m_{cs} for $T_{ci}=5$ °C. The lower the temperature of warm seawater is, the smaller the seawater pipe diameter is needed to obtain the maximum net power. Nevertheless, $(W_n)_{max}$ is larger for a higher T_{ei}.

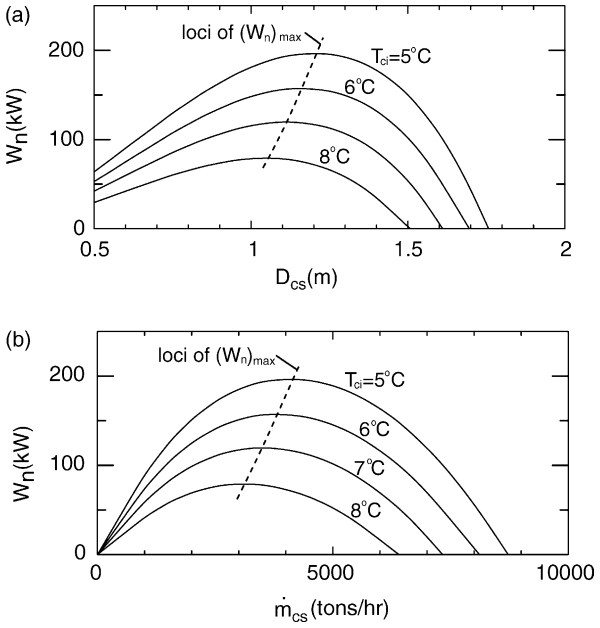

Fig. 9. Dependence of W_n on D_{cs} and m_{cs} for $T_{ci}=5$–8 °C.

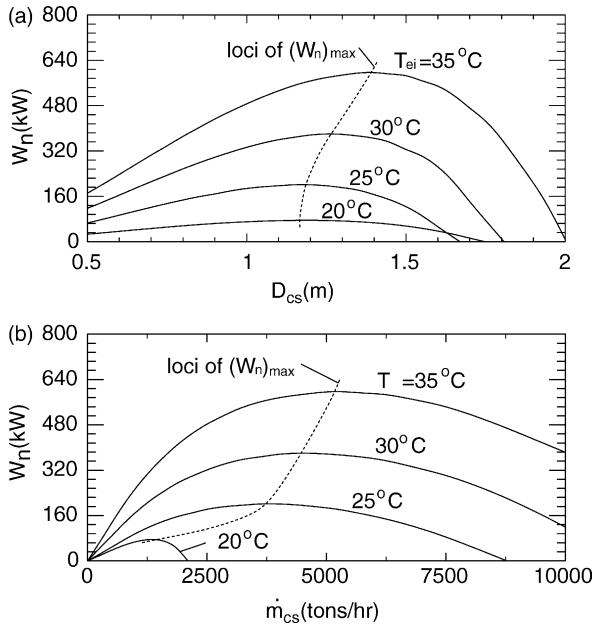

Fig. 10. Dependence of W_n on D_{cs} and m_{cs} for $T_{ei}=20$, 25, 30, and 35 °C.

5. Conclusions

In this study, a theoretical approach is proposed to compute the output powers of an OTEC plant. Assuming either fixed pipe diameter or fixed flow velocity, a maximum generated net power is obtained at a certain mass flow rate of the cold seawater. From the foregoing results, it can be concluded as follows:

1. For fixed D_{cs} and T_{ei}, the lower the temperature of cold seawater is, the higher the maximum net power is obtained.
2. For fixed T_{ei} and T_{ci}, a larger $(W_n)_{max}$ is found for a larger diameter of seawater pipe.
3. For a fixed m_{cs}, the generated net power is increased by increasing m_{ws}.
4. For fixed V_{cs} and T_{ei}, the maximum net power increases with the decrease of T_{ci}. The colder the seawater is, the larger the pipe diameter is used to obtain maximum net power.
5. For fixed V_{cs} and T_{ci}, the maximum net power and its corresponding pipe diameter increase with the temperature of surface warm seawater.

References

Abraham, R., Jayashankar, V., Ikegami, Y., Mitsumori, M., Uehara, H., 1999. Analysis of power cycle for 1 MW floating OTEC plant, Proceedings of International OTEC/DOWA, Imari, Japan 1999, pp. 123–131.

Avery, W.H., Wu, C., 1994. Renewable Energy from the Ocean—A Guide to OTEC. Oxford University Press, Oxford.

Dylan, T., 1995. Ocean thermal energy conversion: current overview and future outlook. Renew. Energy 6 (3), 367–373.

Ganic, E.N., Moeller, L., 1980. Performance study of an OTEC system. Apply Energy 6, 289–299.

Gnielinski, V., 1976. New equation for heat and mass transfer in turbulent pipe and channel flow. Int. Chem. Eng. 6, 359–368.

Nakaoka, T., Uehara, H., 1988a. Performance test of a shell-and-tube plate type evaporator for OTEC. Exp. Therm. Fluid Sci. 1, 283–291.

Nakaoka, T., Uehara, H., 1988b. Performance test of a shell-and-tube plate type condenser for OTEC. Exp. Therm. Fluid Sci. 1, 275–281.

Owens, W.L., 1980. Optimization of closed-cycle OTEC plants, ASME–JSME Thermal Engineering Joint Conference, vol. 2 1980 pp. 227–239.

Petukhov, B.S., Kurganov, V.A., Gladuntsov, A.I., 1973. Heat transfer in turbulent pipe flow of gases with variable properties. Heat Transfer Soviet Res. 5 (4), 109–116.

Rabas, T.J., Panchal, C.B., Stevens, H.C., 1990. Integration and optimization of the gas removal system for hybrid-cycle OTEC power plants. J. Solar Energy Eng. 112, 19–28.

Tseng, C.H., Kao, K.Y., Yang, J.C., 1991. Optimal design of a pilot OTEC power plant in Taiwan. J. Energy Resour. Technol. 113, 294–299.

Uehara, H., Ikegami, Y., 1990. Optimization of a closed-cycle OTEC system. J. Solar Energy Eng. 112, 247–256.

Uehara, H., Kusuda, H., Monde, M., Nakaoka, T., 1979. Ocean thermal energy conversion plant with Freon 22, Proceeding, Sixth OTEC Conference, vol. 6, 1979.

Uehara, H., Miyara, A., Ikegami, Y., Nakaoka, T., 1996. Performance analysis of an OTEC plant and a desalination plant using an integrated hybrid cycle. J. Solar Energy Eng. 118, 115–122.

Yeh, R.H., Su, T.Z., Yang, M.S., 1999. Theoretical analysis of a small-scaled OTEC power plant, Proceedings of International OTEC/DOWA, Imari, Japan 1999, pp. 74–83.